Transactions of the 15th International Conference on
Structural Mechanics in Reactor Technology (SMiRT-15)
Seoul, Korea, August 15-20, 1999

The Prometra Programme: Assessment of Mechanical Properties of Zircaloy 4 Fuel Cladding During an RIA

Marcel Balourdet[1)], Christian Bernaudat[2)], Virginie Basini[3)] and Nicolas Hourdequin[3)]

1) IPSN/DRS/SEMAR, France
2) EDF/SEPTEN, France
3) CEA/DRN/DMT/SEMI, France

ABSTRACT : Hoop and axial tensile tests have been carried out by CEA in order to assess the behaviour of irradiated Zircaloy 4 cladding during Reactivity Initiated Accidents (RIA) : this series of tests, termed PROMETRA, is intended as a support to the programme related to high burnup UO_2 and MOX fuel behaviour in RIA situation, performed by IPSN in collaboration with EDF, using in particular the CABRI reactor in France. Ring and longitudinal samples machined from defueled cladding with up to 130 µm ZrO_2, some of them with spalling, have been tensile tested between 20°C and 1100°C under high strain rate (0.01 to 5 s^{-1}). Ductile failures are usually observed except at low temperatures ($T \leq 150$°C) with moderately corroded cladding and at all temperatures ($T \leq 480$°C) with spalled cladding. For geometrical reasons, stresses within ring samples are far from uniaxial : corrections, based on finite element analysis, are applied to the raw results leading to corrected elongations lower than measured.

SCOPE OF THE PROGRAMME

In France, more than 80% of the electric power generated is now supplied by Nuclear Power Plants (NPPs). Fuel burnup increase is promoted to reduce the cost of energy, which is a great stake for EDF within the next years. However, EDF must assess that the behaviour of high burnup UO_2 and MOX fuel does not lead to core degradation during a design basis reactivity initiated accident (RIA), i.e., in a PWR, a rod control cluster assembly ejection accident leading to fast power increase (in some ms). In this framework, the RIA CABRI REP-Na programme[1] has been run jointly by IPSN and EDF since 1993 with the aim to analyse the high burnup fuel behaviour under RIA transients and to check the relevance of the present safety criterion. In parallel, the PROMETRA (which stands for "Transient Mechanical Properties") programme[1] is devoted to the assessment of the mechanical properties of Zircaloy 4 claddings submitted to fast PCMI transients. It aims at calibrating models for Zircaloy 4 hardening behaviour, including effects of waterside corrosion such as oxidation, ZrO_2 spalling and hydriding. The models will then be implemented into the SCANAIR[1] code in order to better simulate fuel behaviour during accidents.

During an RIA, following energy injection in the fuel, the cladding is loaded rapidly by thermal expansion of the fuel pellets, possibly reinforced by pressurisation of the fission gases within fuel pores ; afterwards, depending on conditions in the coolant channel, a slower process (plenum pressure driven clad ballooning) may occur. Presently, we are only interested in the first phase of the accident which is dominated by Pellet Clad Mechanical Interaction (PCMI) : it is characterised by fast heating rates, about 10^3 K. s^{-1}, and by high strain rates,

typically 1 s^{-1} as observed during CABRI tests ; starting from hot zero power, the cladding may reach any temperature above 280°C but values up to 600°C are of prime interest for the PCMI phase ; also, colder conditions, down to room temperature, are of interest for the interpretation of power burst tests in the Japanese NSRR reactor. The cladding is submitted to axial as well as to hoop stresses with a ratio σ_z / σ_θ between 0.5 (pure gas pressure) and 1 (pure PCMI). The cladding of interest is cold worked and stress relieved Zircaloy 4 irradiated for 5 cycles in commercial NPPs up to about 60 GWd/t local burn up. For the reactor case, the outer oxide layer should not exceed 100 µm without any spalling but more severe corrosion and spalling have been considered too.

Clad mechanical testing should aim mainly at providing behaviour laws, i.e. strain hardening laws as a function of relevant parameters (transient loading conditions and initial state of the cladding resulting from the base irradiation), enabling the transient response to be predicted by computer codes such as SCANAIR, i.e. how much the cladding deforms and how it reacts on the pellet. Thus, a series of, hopefully uniaxial, tensile tests on machined specimens has been preferred in spite of their shortcomings such as non-uniform stress and strain fields and as the lack of representativity with respect to the tubular geometry of the actual rod. Additionally, a failure criterion should be set up. Also, mechanical testing should help understanding how some early and brittle rod failures could occur in CABRI, for instance in REP-Na 1 (Tab. 1) and in NSRR (HBO-1 test), i.e. the Ductile-Brittle Transition (DBT) is to be addressed.

TENSILE TEST CONDITIONS AND RESULTS

Test Matrix

Most samples studied stem from spans 2 to 6 of rods equipped with cladding of an old design (about 1.5 % Sn) and irradiated 5 cycles ; some have been taken in span 2 of a rod with low Sn cladding irradiated only up to 4 cycles. They are characterised by the ZrO_2 thickness as measured on the rods themselves or on twin rods by an eddy current technique. Short rod segments (6 cm for tensile tests, 12 cm for burst tests) are chemically defueled and the outer ZrO_2 layer is mechanically removed to allow the subsequent spark machining of specimens with three geometries : hoop specimens consisting of small rings with two slender parts providing a 3 mm gauge length in the transverse direction (Fig. 1, 6 & 12) ; long axial specimens with 15 mm gauge length in the rolling direction ; short axial specimens with only 5 mm gauge length in the rolling direction but with a thermocouple spot-welded on one of the gauge parts (Fig. 2 & 11). The latter ones can be heated up rapidly, at 100 $K.s^{-1}$, by an electric current passing through the cladding (it has been checked that higher heating rates were not needed). The first two types are heated in a furnace at only 0.2 $K.s^{-1}$ heating rate. Specimen dimensions are measured before testing.

Hoop specimens are placed around two half-cylinder inserts which are attached to the cross-heads and pulled apart inside the rings. Axial specimens can be stretched by pins attached to the cross-heads and passing through the cladding and through bored end caps. In both cases, the fixtures are placed in a servohydraulic tensile test machine equipped with load and displacement sensors on the cross-head ; data acquirement and test parameter control are ensured by a small computer. A cross-head displacement at constant velocity is triggered once the desired test temperature is reached either slowly (with hoop and with long axial specimens) or rapidly (with short axial specimens). After test, pictures are taken and samples can be examined by optical microscopy or by Scanning Electron Microscopy (SEM). In addition, a few burst tests are performed on, chemically defueled, 12 cm long tubes. Due to sample availability, many hoop tests could be performed, allowing for a rather consistent test

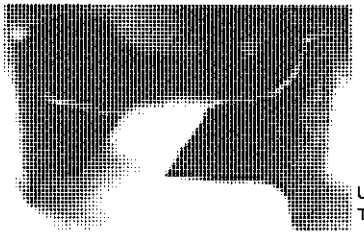

Fig. 1 : failed hoop specimen

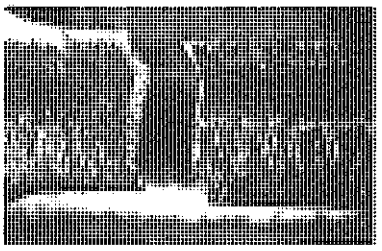

Fig. 2 : detail of failed axial specimen

Table 1 : Main characteristics of CABRI REP-Na experiments

Experiment	REP-Na 1	REP-Na 7	REP-Na 8	REP-Na 9	REP-Na10
Fuel (GWd/t)	UO_2 – 64	MOX – 55	UO_2 – 60	MOX – 28	UO_2 – 62
Max. ZrO_2 (µm)	90 – spalled	50	130 – spalled	12	90 – spalled

Table 2 : Tensile test matrix showing temperature ranges (in °C) covered by the different specimen types and cladding conditions (all tests at 0.01 and 5 s^{-1}, some at 0.2 s^{-1}).

Type of Specimen	Heating Rate ($K.s^{-1}$)	State of the Cladding (ZrO_2 thickness in µm)				
		Unirradiated	< 30 µm	30 to 60	60 to 100	> 100 µm
Hoop	0.2	20 - 600	280 - 600	20 - 600	280 - 600	280 - 480
Long Axial	0.2	280 - 800	280 - 800	280 - 700	280 - 700	
Short Axial	100	600 - 1100		700 - 1100		

matrix (Tab. 2) with a wide range of temperatures (20 to 600°C) and of corrosion levels (0 to 130 µm ZrO_2 thickness). On the other hand, axial tests were not numerous enough in view of the temperature range covered (280 to 1100°C) and less corrosion levels have been covered ; axial results have been published elsewhere[2]. Therefore, we shall concentrate on hoop tests : these are also more representative of PCMI loading.

Anisotropy (Hoop And Axial Tests)

As far as the 0.2% offset yield stress (YS) and the ultimate tensile strength (UTS) are concerned, the difference between hoop and axial results is negligible with respect to the scatter of data. A clear apparent anisotropy is displayed by the uniform elongation (UE), axial values being about twice larger than the hoop ones. Total elongations (TE) from long axial specimens are apparently smaller than those from hoop tests but this is due to the larger gauge length (L_0 = 15 vs. 3 mm), the corresponding displacements ($TE \times L_0$) being similar.

Strain Rate And Temperature (Hoop Tests)

The resistance (UTS on Fig. 3 and YS) decreases with increasing temperature and with decreasing strain rate with a small strain rate sensitivity ($\partial Log UTS / \partial Log \dot{\varepsilon} \approx 0.03$). Assuming a strain hardening law of the type $\sigma = \sigma_0 \varepsilon^N$, strain hardening coefficients can be crudely estimated from the measured YS, UTS and UE : no clear influence of temperature or strain rate is observed with a mean value $N \approx 0.05$, smaller than axial values (0.05 to 0.1).

UE values are to be considered with caution (Fig. 4) : they become much higher above 550°C as a result of pre-test annealing due to the slow heating rate ; indeed, recristallization and complete hydride redistribution have been evidenced by micrography of specimens tested

at 600°C. This applies to axial tests too with a maximum UE towards 700°C : only short axial samples, i.e. tested after transient heating, exhibit high temperature UE values similar to the low temperature ones. Another question is raised by 4 cycle irradiated low Sn cladding : its UE is larger than that of the standard material, especially above 350°C and at high strain rate : this seems to be a peculiarity of the low Sn cladding (also, it seems less prone to embrittlement by hydrides as suggested by tests carried out by EDF on unirradiated samples). Thus, if low Sn cladding as well as annealed samples ($T \geq 550°C$) are excluded, the UE of standard and non-spalled cladding does not vary significantly with temperature and it decreases only slightly with strain rate : exceptions are extremely corroded ($ZrO_2 \approx 130$ µm) and spalled samples from the same rod as the one used in CABRI REP-Na 8 (Tab. 1). The TE increases linearly with temperature and it decreases with strain rate (Fig. 9).

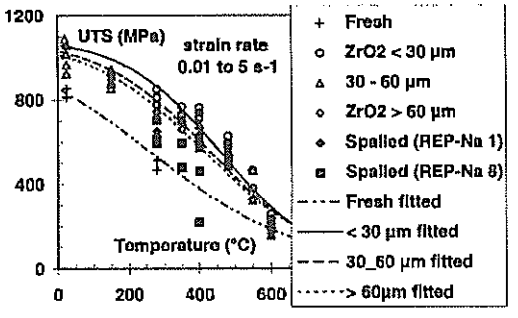

Fig. 3 : hoop UTS versus temperature

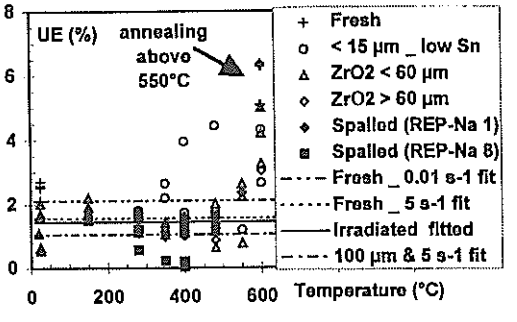

Fig. 4 : hoop UE versus temperature

Irradiation And Corrosion (Hoop Tests)

Irradiation results in a strong increase of the resistance (UTS on Fig. 3 and YS) which is best displayed by samples with the lowest corrosion ($ZrO_2 \leq 20$ µm). Some influence of the irradiation temperature is to be seen in the low temperature range ($T \leq 150°C$) on samples with the same, medium, corrosion ($ZrO_2 \approx 45$ µm) : those from a lower span (low irradiation temperature) have a greater resistance. As long as there is no spalling, UTS and YS decrease steadily with increasing corrosion suggesting a loss of resistance from a thicker hydride rim. Spalled samples behave differently : most of them compare with non-spalled cladding at the same corrosion ; other ones, even the majority for REP-Na 8 type cladding (Tab. 1), have a considerably reduced UTS (Fig. 3), down to less than half the "non-spalled" value : this is consistent with the presence of hydride blisters with about half the cladding thickness, as observed with the REP-Na 8 micrography (Fig. 5). Such samples are also characterised by brittle failures with quite small elongations. In the case of REP-Na 1 type cladding (Tab. 1), blisters occupy only one third of the thickness, hence the reduced influence on the resistance.

If untypical results due to annealing are omitted, the UE of non-spalled cladding seems close to that of the unirradiated material in view of the scarcity of data ; only highly corroded samples ($ZrO_2 \approx 80$ µm) have a slightly lower UE (1% instead of 1.5%) when tested at the highest strain rate ($5\ s^{-1}$) ; highly corroded and spalled cladding, such as it has been used in REP-Na 1 does not differ in that respect. For extremely corroded and spalled cladding, i.e. REP-Na 8 type, results are extremely scattered : in some cases, no plastic deformation has been recorded and the failure occurred outside the gauge and fillet zone. The TE of irradiated but non-spalled cladding is lower, particularly at room temperature, than that of the fresh material tested at the same strain rate but it does not seem to depend on the degree of

corrosion. The ductility of spalled cladding is severely reduced (see DBT item).

Strain Energy Density (Hoop Tests)

Plastic Strain Energy Densities (SED) can be estimated by integrating the engineering stress-strain curves. Depending on the loading conditions in an RIA, two critical SED values have to be considered either up to necking onset ($CSED_{UE} \approx$ UTS x UE) or up to failure (the second one has little significance because the deformation is then concentrated in the, unknown, necking zone). If non-typical results are excluded (low Sn, etc.), the $CSED_{UE}$ reflects mainly the decrease of the UTS with temperature and corrosion ; again, REP-Na 8 type samples yield values scattered between zero and the level of non-spalled cladding.

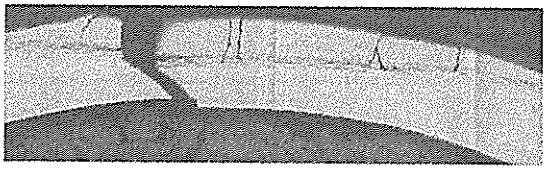

Fig. 5 : CABRI REP-Na 8 micrography

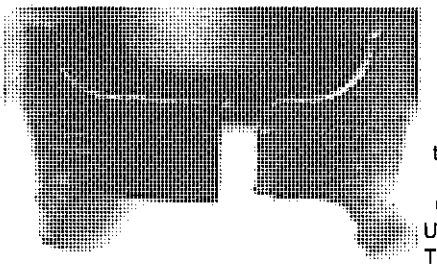

Fig. 6 : CABRI REP-Na 1 type cladding

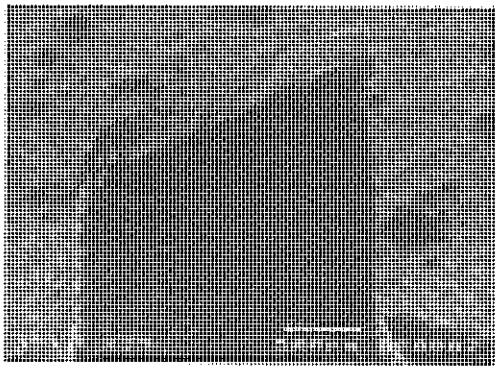

Fig. 7 : SEM of ductile sample on Fig. 1

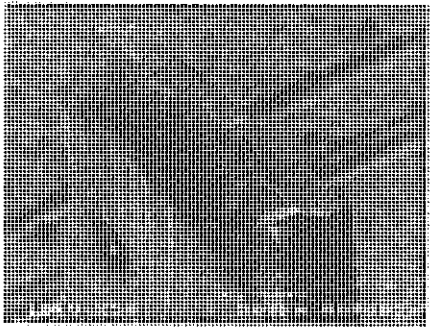

Fig. 8 : SEM of brittle sample on Fig. 6

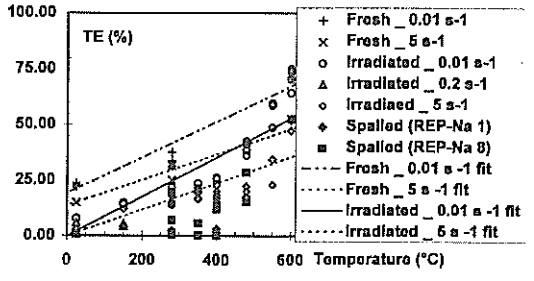

Fig. 9 : hoop TE versus temperature

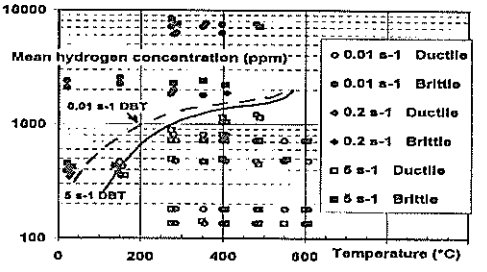

Fig. 10 : tentative DBT map

Ductile-Brittle Transition (Hoop Tests)

The failure mode is best determined from the post-test appearance of a specimen as seen globally by visual examination and locally by optical microscopy or by SEM. Whenever the

latter examinations are carried out, faceted structures are to be found on fracture surfaces perpendicular to the stress direction whereas ductile aspects with dimples are to be seen on slant surfaces : the latter features can be observed through the width of ductile specimens (Fig. 7) but also, with shallow dimples, through the thickness of brittle specimens towards the inner cladding region, brittle structures being limited to the outer rim (Fig. 8). Similar distributions have been observed on spalled plain rings tested by CEA-Grenoble[1] and after the CABRI REP-Na 1 experiment[1] carried out with a spalled rod having up to 90 µm ZrO_2 (Tab. 1). After another experiment (REP-Na 8 – Tab. 1) with a spalled rod and even higher corrosion (up to 130 µm), brittle cracks are to be seen going through a hydride blister, one of them going through the inner cladding layers in a ductile manner (Fig. 5). Similar observations have been done after the HBO-1 and HBO-5 NSRR experiments[3].

As far as tensile data are concerned, the quantity which is best correlated with the failure mode is the necking strain (TE - UE) : it becomes negligibly small in case of brittle failure, especially with spalled cladding. As many low temperature tests on non-spalled cladding led to brittle failures, it can be stated that, for such samples with medium corrosion, the DBT temperature is higher than room temperature at 0.01 s^{-1} strain rate and close to 200°C at 5 s^{-1} strain rate (Fig. 10). Spalling results in a strong scatter : some tests end up with a ductile failure with a slant crack (Fig. 1 & 7) and with the same TE as in the non-spalled case ; others give way to brittle failure with a crack perpendicular to the tensile stress (Fig. 6 & 8) and with a TE hardly greater than the UE. Metallographic examinations are underway in order to check the most likely explanation, i.e. that the embrittlement is correlated to the presence of a hydride blister as already observed on plain rings tested at CE-Grenoble[1] (it is still undecided whether non-spalled cladding with 130 µm ZrO_2 may not be brittle at 280°C). Figure 10 summarises failure modes on a hydriding-temperature plot ; with spalled and brittle specimens, the presence of a blister has been assumed for estimating thickness averaged hydrogen contents. The important result is that, under hot zero power conditions of French NPPs ($T \geq 280$°C), non-spalled cladding with less than 100 µm ZrO_2 remains ductile. On the other hand, brittle failures cannot be avoided during NSRR experiments starting from room temperature.

FINITE ELEMENT MODELLING OF TENSILE SPECIMENS

Hoop and axial tensile tests should aim at measuring uniaxial properties either in the transverse or in the rolling direction. However, the designs of machined samples used by CEA are far from those of normalised specimens so that the results suffer from adverse effects : in the course of a test, especially with a ring, the gauge portions move towards the cladding axis giving way to unwanted bending ; even if steps are taken to maintain a constant sample curvature, strains are never distributed uniformly in the gauge parts due to boundary conditions with a limited sample width, as demonstrated at the University of Pennsylvania[4]. It is therefore necessary to evaluate the consequences of such artefacts and to try and correct experimental results in order to estimate what constitutive laws would apply to undisturbed situations. Thus, Finite Element Analyses (FEA) have been carried out by CEA-Saclay with the CASTEM 2000 code assuming isotropic plasticity and a single constitutive equation through the thickness although irradiated cladding is far from homogeneous. Thanks to symmetry, only $1/8^{th}$ of samples need be modelled with cubic meshes (4 over the thickness, 4 to 7 over a half-width and 20 along a quarter circumference). Friction between a machined hoop sample and the die inserts can be neglected as shown by exploratory calculations.

It appears that the plastic strain field is homogeneous within most of the gauge parts of axial samples (Fig. 11) : such tests can be considered as actually uniaxial and constitutive

laws can be derived straightforwardly from the load-displacement curves. In contrast, bending stresses in hoop samples are about as high as membrane stresses ; as a result, plastic strains are concentrated in the middle of the gauge parts and on the inner clad surface with strong variations across the thickness (Fig. 12) : results from hoop tests cannot be used directly.

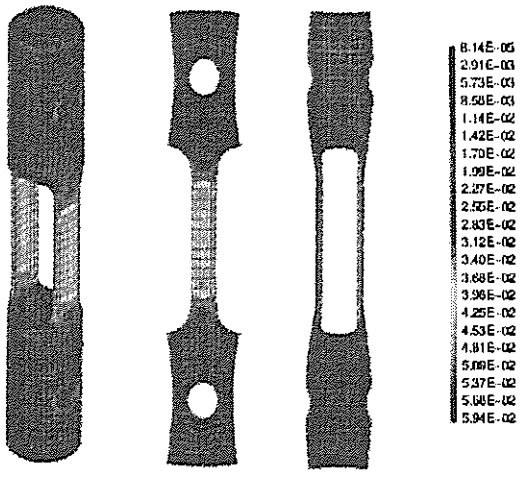

Fig. 11 : effective plastic strain distribution in an axial sample at necking onset

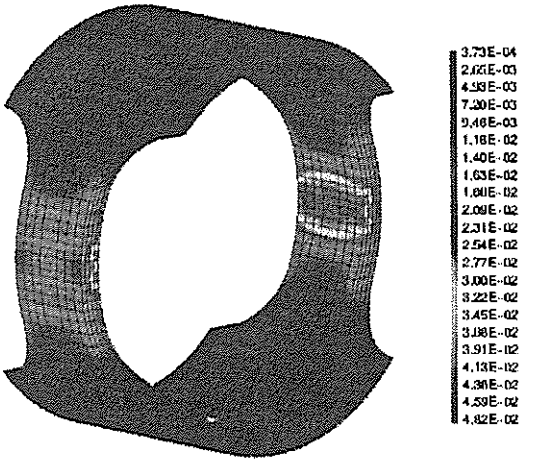

Fig. 12 : effective plastic strain distribution in a hoop sample at necking onset

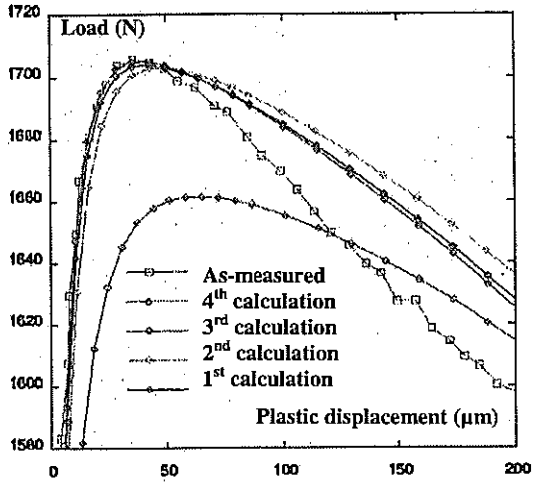

Fig. 13 : calculated versus measured load-displacement curve

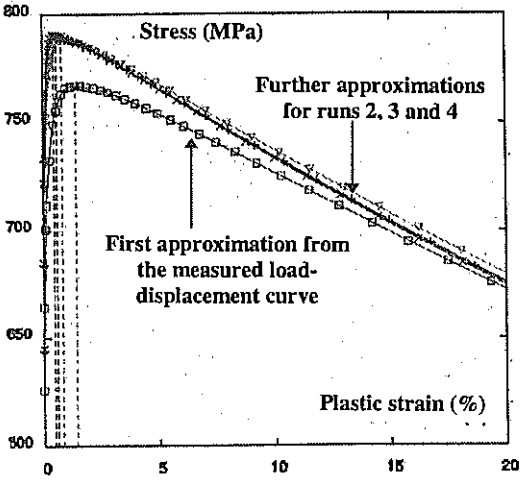

Fig. 14 : engineering representation of iterated constitutive equations

An iterative procedure is employed for reconstructing a constitutive law from a hoop test. True stresses and true plastic strains, deduced from the as-measured tensile curve, are used up to necking onset and extrapolated to higher strains by a power law ($\sigma = \sigma_0 \varepsilon^N$) : this is taken, together with known elastic constants, as a first approximation of the constitutive equation for a first run of CASTEM. The FEA calculated load-displacement curve is compared with

the as-measured one (Fig. 13) and the first law is modified accordingly, by factors characterising the ratios between measured and calculated responses, and fed back into the code as a second approximation for a further calculation. Discrepancies stabilise after a few runs and the last behaviour law is considered as the "real" constitutive law (Fig. 14).

Applied to cladding with little corrosion, which is influenced mainly by the irradiation, the corrective procedure results in a slight increase of the UTS (by a few %) and in a significant decrease, more important at low temperature than at high temperature, of the UE. The same method can be used with more corroded cladding but an alternative procedure under study would be to reduce the cladding thickness in order to simulate the loss of strength from a hydride rim and to keep the constitutive equation of cladding with little corrosion for the "sound" layers ; application of this procedure to sets of tests with different corrosion thicknesses is in progress. However, this alternative method may not be so straightforward because it is based on the assumption that corrosion and "sound" cladding behaviour are independent even though both depend on the irradiation temperature.

CONCLUSION

Transient mechanical properties of high burnup Zircaloy 4 cladding are mainly influenced by the waterside corrosion as shown by axial and mainly hoop tensile tests. As long as there is no spalling, the ductility compares with that of the fresh material and the cladding is ductile under RIA conditions. In case of spalling, with the likely formation of hydride blisters, the cladding is brittle, at least up to 480°C, with a negligible ductility (zero necking strain) and with a strongly reduced strength. An iterative FEA procedure has been developed for estimating behaviour laws from raw results of hoop tests in spite of their highly heterogeneous stress and strain fields. Strictly speaking, such laws are not the real constitutive equations which would apply to purely uniaxial tension ; but they are practical approximations for the description of the biaxial loadings which are experienced by ring samples during tests or by actual rods during an accident and which result in very small uniform elongations close to those from burst tests (0.25 %). However, such low values can be considered as the limit strain only in case of either a sustained pressure source, as assumed for CABRI REP-Na 7 with MOX fuel (Tab. 1), or if the cladding has been embrittled due to spalling (REP-Na 1, 8 & 10 – Tab. 1). In all other cases (PCMI loading, even with a limited gas contribution which can be relieved by the slightest rod deformation) the necking strain provides a large enough ductility margin before failure (REP-Na 9 withstood more than 8 % hoop strain).

REFERENCES

1. Papin, J., Balourdet, M., Lemoine, F., Lamare, F., Frizonnet, J.M., and Schmitz, F., "French Studies on High-Burnup Fuel Transient Behavior Under RIA Conditions," *Nuclear Safety*, Vol. 37 No. 4, 1996, pp. 289-327.
2. Balourdet, M., and Bernaudat, C., "Tensile Properties of Irradiated Zircaloy 4 Cladding Submitted to Fast Transient Loading," *Proc. of the CSNI Specialist Meeting on Transient Behavior of High Burnup Fuel*, pp. 417-431, Cadarache France, September 1995.
3. Fuketa, T., Nagase, F., Ishijima, K., and Fujishiro, T., "NSRR/RIA Experiments with High-Burnup PWR Fuels," *Nuclear Safety*, Vol. 37 No. 4, 1996, pp. 328-342.
4. Link, T.M., Koss, D.A., and Motta, A.T., "Failure of Zircaloy Cladding under Transverse Plane-Strain Deformation," *Nuclear Engineering and Design*, Vol. 186, 1998, pp. 379-394.